

Electrical transport in disordered and ordered magnetic domains under pressures and magnetic fields

This article has been downloaded from IOPscience. Please scroll down to see the full text article.

2009 J. Phys. D: Appl. Phys. 42 032006

(<http://iopscience.iop.org/0022-3727/42/3/032006>)

View [the table of contents for this issue](#), or go to the [journal homepage](#) for more

Download details:

IP Address: 38.107.179.212

The article was downloaded on 22/02/2012 at 06:54

Please note that [terms and conditions apply](#).

FAST TRACK COMMUNICATION

Electrical transport in disordered and ordered magnetic domains under pressures and magnetic fields

J A Souza¹ and R F Jardim²¹ Centro de Ciências Naturais e Humanas, Universidade Federal do ABC, CEP 09090-900, Santo André, SP, Brazil² Instituto de Física, Universidade de São Paulo, CP 66318, 05315-970, São Paulo, SP, BrazilE-mail: joseantonio.souza@ufabc.edu.br

Received 18 September 2008, in final form 10 December 2008

Published 9 January 2009

Online at stacks.iop.org/JPhysD/42/032006**Abstract**

Magnetic $M(T, H, P)$ and electrical transport $\rho(T, H, P)$ measurements in a strong spin–lattice–charge coupled $\text{La}_{0.7}\text{Ca}_{0.3}\text{MnO}_3$ system have been conducted. The application of H and P leads to the formation of different magnetic domain structures in the vicinity and below the polaronic-to-ferromagnetic transition temperature. The charge mobility is more sensitive to the variation of the spatial wave function overlap between $\text{Mn}^{3+} e_g$ and $\text{O}^{2-} 2p$ orbitals due to the applied compacting pressure rather than the relative spin orientation between neighbouring Mn ions when the magnetic field is applied. In spite of the presence of different magnetic domain structures due to the sample history, the effect of magnetic field and pressure is less pronounced at lower temperatures on electrical transport properties.

Doped manganese oxides exhibit a strong interplay between lattice, charge and spin degrees of freedom. As a result of coupling between them, interesting physical effects take place when thermodynamic parameters such as pressure (P), magnetic field (H) and temperature (T) are varied [1]. Indeed, magnetocaloric (MC), magnetostriction (MS), colossal magnetoresistivity (MR) and pressure-resistivity (PR) effects observed in these compounds have been a subject of great interest in condensed matter physics [2]. These effects are much more pronounced in the vicinity of the magnetic, structural and electronic phase transitions where phase coexistence and the correlation length can be easily altered depending on their nature. The compound $\text{La}_{0.7}\text{Ca}_{0.3}\text{MnO}_3$ exhibits a continuous *polaronic*-to-ferromagnetic (FM) phase transition [3] with an unusually large critical exponent revealing close proximity to the phase boundary where second order transitions become first order (or nearly first order). At high temperatures, these polarons behave like paramagnetic entities with an uncorrelated and complex order parameter and exhibit a semiconducting like charge mobility.

A change in the electronic conductivity from polaron gas (adiabatic) to polaron liquid (nonadiabatic) was found in this $\text{La}_{0.7}\text{Ca}_{0.3}\text{MnO}_3$ compound at a high temperature [4]. Such a correlated polaronic structure is believed to be a precursor of the low temperature FM and metallic state where MR and PR are robust.

The metallic-like electronic conduction in the FM state at low temperatures is described by the double exchange (DE) interaction [5]. Accordingly, the strength of the DE interaction depends on the charge carrier transfer integral $t = t_0 \cos(\theta/2)$, which depends on both the spatial wave function overlap t_0 and the relative angle between two neighbouring Mn ion spins θ . The quantity t_0 is proportional to the bandwidth (W), which in turn depends on structural parameters $W = \cos(\omega)/(d_{\text{Mn-O}})^{3.5}$, where $\omega = \frac{1}{2}(\pi - \langle \text{Mn-O-Mn} \rangle)$ is the tilt angle in the plane of the bond and $d_{\text{Mn-O}}$ is the Mn–O bond length [6]. Both magnetic field and applied pressure induce qualitatively similar effects stabilizing the FM metallic phase [7]. The mechanisms through which both P and H improve charge mobility are different. The magnetic field

favours the spin alignment, changes the angle between spins, which increases the electron hopping rate bringing about the MR effect. On the other hand, the effect of pressure is to alter the structural parameters by compressing the Mn–O distance and increasing the Mn–O–Mn bond angle, leading to a variation in the spatial function overlap— $\text{Mn}^{3+} e_g$ and $\text{O}^{2-} 2p$ orbitals—the bandwidth.

In this work we focus our attention on the electrical resistivity $\rho(T, H, P)$ and magnetization $M(T, H, P)$ as a function of temperature when a magnetic field and hydrostatic pressure are applied in the vicinity of the polaronic-to-FM transition in $\text{La}_{0.7}\text{Ca}_{0.3}\text{MnO}_3$. We systematically compare and discuss the MR and PR effects across the phase transition. The charge mobility below the percolation threshold (in the metallic state) where DE is operative is much more sensitive to the variation of the spatial wave function overlap between Mn–O–Mn orbitals than the relative spin angle between neighbouring Mn ions.

Four-probe electrical resistivity $\rho(T, H, P)$ was measured in magnetic fields and under hydrostatic pressures. For pressure measurements, we used a beryllium–copper self-clamping device with Fluorinert as a pressure transmitting medium. Magnetization $M(T, H, P)$ measurements [9] were performed in a commercial superconducting quantum interference device (SQUID) magnetometer. A dense polycrystalline sample of $\text{La}_{0.7}\text{Ca}_{0.3}\text{MnO}_3$ was prepared through a sol–gel method [3, 8]. Based on sintering and annealing temperatures and compared with a number of previous studies [1, 2] that have looked at grain size dependence on physical properties, we estimated a grain size of $\sim 15 \mu\text{m}$ for our sample indicating little grain boundary effect. On the other hand, large grains promote a multidomain regime with the presence of domain walls which is expected to act strongly as scattering centres.

Figure 1(a) shows electrical resistivity and magnetization (inset) as a function of the temperature in the presence of magnetic fields. An electronic phase transition from insulating (localized carriers) to metallic (itinerant carriers) takes place simultaneously to the FM phase transition at $T_{\text{MI}} = 259.7 \text{ K}$, defined as the temperature where $d\rho/dT = 0$. This is actually confirmed in the inset of figure 1(a) where the temperature dependence of the magnetization is displayed; an FM transition takes place at $T_c = 250 \text{ K}$, defined as the temperature where dM/dT is minimum. The application of a moderate magnetic field H reduces the electrical resistivity of the system. Such a decrease in ρ is caused by the improvement in the alignment of spins which, in turn, enhances the bandwidth and shifts both T_c and T_{MI} to higher temperatures [10]. These results indicate a strong coupling between *spin* and *charge* in $\text{La}_{0.7}\text{Ca}_{0.3}\text{MnO}_3$. Besides the spin–charge coupling, we have measured electrical resistivity and magnetization under pressure in order to probe both the *charge–lattice* and the *spin–lattice* couplings, as shown in figure 1(b). In a very similar fashion, the application of pressure results in a shift of both T_{MI} and T_c to higher temperatures, further demonstrating the relevance of the charge–lattice and spin–lattice couplings, respectively. Increasing the applied pressure also reduces the electrical resistivity of the system. Applying pressure results

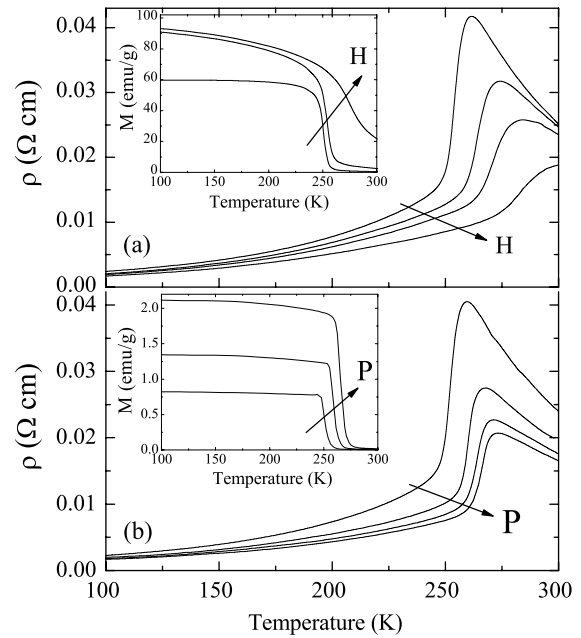


Figure 1. (a) Temperature dependence of the electrical resistivity under magnetic fields of $H = 0, 20, 30$ and 50 kOe . The inset displays magnetization measured at $H = 1, 5$ and 50 kOe and at the ambient pressure. (b) Temperature dependence of the electrical resistivity under pressures of $P = 0, 0.59, 0.91$ and 1.18 GPa . The inset shows some selected magnetization curves measured at $P = 0, 0.28$ and 0.73 GPa and in the presence of $H = 10 \text{ Oe}$.

in a decrease in the unit cell volume and an increase in the exchange interaction between $\text{Mn}^{3+}/\text{Mn}^{4+}$ pairs. The lattice structural compression in both the Mn–O bond distance and the Mn–O–Mn bond-angle is believed to change the spatial wave function overlap. The net result is the strengthening of the DE interaction and a shift of T_{MI} to higher temperatures. All the results discussed above are in agreement with the literature [1, 11–13].

The temperature dependence of both MR and PR effects for different magnetic fields and applied pressures is displayed in figure 2. Overall, both effects are stronger close to T_c ; the PR effect is more symmetric. However, the MR is much more robust than the PR effect in the high temperature polaronic state. More interesting is the temperature dependence of PR shown in figure 2. The dashed line indicates T_{MI} ($d\rho/dT = 0$) of the virgin curve ($P = 0$ and $H = 0$) and the stars T_{MI} in the presence of pressure of $P = 0.59, 0.91$ and 1.18 GPa . Note that above T_{MI} the PR effect is almost temperature independent, increasing smoothly below the percolation threshold, where polarons coalesce and form long-range FM domains. An estimation of the polaron energy just above T_{MI} (marked by stars in figure 2) taking into account the small polaron mechanism [4, 14] as a function of pressure yields $E_p = 0.117 \text{ eV}, 0.107 \text{ eV}, 0.095 \text{ eV}$ and 0.091 eV for $P = 0 \text{ GPa}, 0.59 \text{ GPa}, 0.91 \text{ GPa}$ and 1.18 GPa , respectively. E_p is closely related to the DE bandwidth [15] which depends on both the Mn–O distance and the Mn–O–Mn bond angle. Therefore, this result further indicates that the wave function overlap between Mn and O orbitals was changed in the paramagnetic/semiconducting phase. On the other hand,

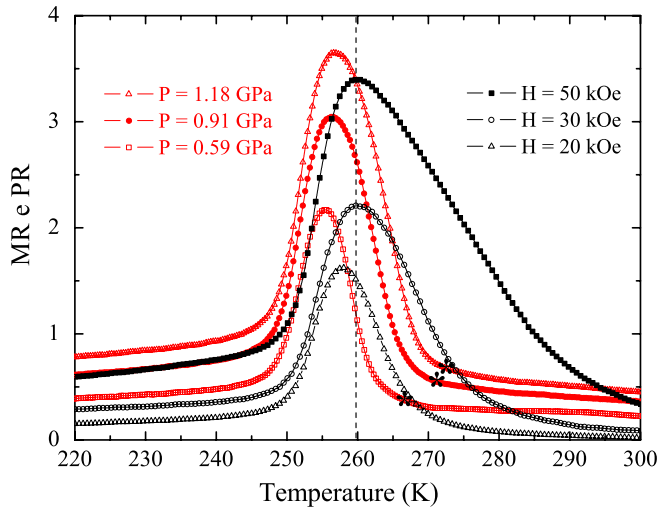


Figure 2. Temperature dependence of the magnetoresistivity, $MR = [\rho(T, H = 0) - \rho(T, H)]/\rho(T, H)$ and pressure-resistivity, $PR = [\rho(T, P = 0) - \rho(T, P)]/\rho(T, P)$ in $La_{0.7}Ca_{0.3}MnO_3$ in the vicinity of the metal-insulator transition T_{MI} . The dashed line indicates $T_{MI}(P = 0, H = 0) = 259.7$ K and the stars indicate $T_{MI}(H = 0) = 267.6$ K, 271.5 K and 272.9 K under applied pressure of $P = 0.59$ GPa, 0.91 GPa and 1.18 GPa, respectively.

(This figure is in colour only in the electronic version)

the temperature dependence of the MR effect is less sensitive to the coalescence of polarons across the percolation threshold. This result indicates that the decrease in the electrical resistivity of the system is caused mainly by the decrease in the magnetic scattering centres and an application of H favours the short-range order coalescence of polarons. The net result is a concomitant suppression of the random spin fluctuations. In fact, the MR effect occurs in two stages: (i) a rotation of the polarons in the H direction due to the magnetic energy (μH) and (ii) a pronounced increase in M at high H (see inset of figure 1(a)) due to the growth of polarons through overlap (magnetic exchange energy), and their eventual formation into large FM domains at lower temperatures [16]. In the case of the PR effect, we show here that the first stage is absent (see figure 2, PR is temperature independent above the T marked by star)—the polaron overlap is dominant due to the applied compacting pressure favouring magnetic exchange.

Overall, the magnitude of MR and PR below T_c (metallic phase) is comparable. In particular, we have found that PR at $P = 0.91$ GPa and MR at $H = 50$ kOe have the same magnitude below ~ 257 K, as can be seen in figure 2. Below ~ 250 K, both curves coincide. This suggests that below T_c the electrical resistivity has exactly the same magnitude in both environments: $P = 0.91$ GPa and $H = 0$ and $P = 0$ and $H = 50$ kOe. In a percolative picture, the electrical resistivity behaviour arises from the magnetic field and temperature dependent concentration of FM metallic regions within an insulating background [17]. A paramagnetic and insulating component coexists with the ordered phase down to 20 K [18]. A higher volume fraction of the metallic phase would result in a lower electrical resistivity of the system. Since the

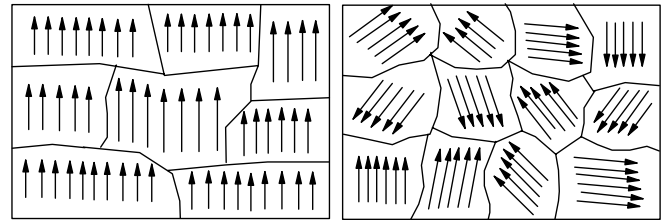


Figure 3. Schematic picture illustrating magnetic domains near and below T_c under: (left) $P = 0$ and $H = 50$ kOe. (right) $P = 0.91$ GPa and $H = 0$. The distance between the arrows represents how compact are the domains comprising magnetic ions.

metallic state stems from the FM-ordered spin alignment through the DE mechanism, the magnitude of the electrical resistivity is expected to follow the magnitude of the magnetic moment near and below T_c . Hundley *et al* [19] proposed that electrical resistivity and magnetism, near and below T_c , follow a phenomenological exponential expression ($\ln(\rho) \propto -M$) in $La_{0.7}Ca_{0.3}MnO_3$. Our results point out that this relation is not straightforward and should be interpreted with care when different magnetic domain structures are under pressure and/or magnetic fields.

The insets of figures 1(a) and (b) show that the magnitude of the magnetic moment at $T = 200$ K reaches 82 emu g^{-1} and 2.1 emu g^{-1} in the presence of $H = 50$ kOe ($P = 0$) and $P = 0.73$ GPa ($H = 10$ Oe), respectively. Bulk magnetization measurements depend on both the *local ordered moment* and the *magnetic domain structure*. Based on the above values of the magnetic moment we draw an illustrative picture of the metallic and FM domains at low temperatures, as depicted in figure 3. As the configuration under $P = 0.73$ GPa ($H = 10$ Oe) has a smaller magnetic moment (2.1 emu g^{-1}), the magnetic domains are expected to be randomly aligned, a more disordered structure. This value, 2.1 emu g^{-1} , would have been smaller if we had measured magnetization in zero magnetic field. On the other hand, when a high magnetic field is applied, $H = 50$ kOe ($P = 0$), the magnetic domains orient to the field growing in size and decreasing in number, resulting in a higher saturation magnetization (82 emu g^{-1}), as seen in figure 3. Interestingly, both disordered and ordered magnetic domains systems have the same magnitude of the electrical resistivity or the MR/PR effect, as shown in figures 1 and 2. This remarkable result indicates that the magnetic domains (core) at $P = 0.91$ GPa ($H = 0$) have a higher electrical conductivity than those at $H = 50$ kOe ($P = 0$) to compensate the scattering of the charge carriers at the domain walls or disordered interfaces [20, 21]. In spite of a very different domain structure at lower temperatures (below ~ 140 K), all curves in figures 1(a) and (b) have the same magnitude regardless of the presence of H or P , indicating mainly that magnetic rotation is negligible. The magnetic rotation effect starts to be pronounced above ~ 150 K. This effect becomes very robust as T_c is approached from below. It is in line with the model by Zhang and Yang [22] where the CMR effect is related to the presence of thermally activated magnetic domains whose average size depends on temperature and magnetic field.

Based on these combined results we assert that below and in the vicinity of T_c the charge transfer is more sensitive to the variation of the spatial overlap between Mn–O–Mn orbitals (pressure effect) than the relative spin orientation. Loa *et al* [23] showed that a bandwidth-driven insulator–metal transition is observed even in the pure LaMnO_3 system as the pressure is increased. More recently, Fuhr *et al* [24] obtained the evolution of the electronic structure showing that the gap closes with pressure in a way similar to that observed by the temperature dependence of the conductivity. In all the cases, the pressure strongly influences the overlap between $\text{Mn}^{3+} e_g$ and $\text{O}^{2-} 2p$ orbitals—the bandwidth.

In summary, we have studied here the couplings between spin–charge, spin–lattice and charge–lattice in the prototype $\text{La}_{0.7}\text{Ca}_{0.3}\text{MnO}_3$ compound and compared the magnetoresistivity and pressure-resistivity effects near and below T_c . We have observed that both $P = 0.91$ GPa ($H = 0$) and $H = 50$ kOe ($P = 0$) environments lead to the same net change on the electronic transport in the metallic state, where DE is operative. These environments brings about different magnetic domain structures. Taking into account strong scattering at domain walls, we suggest that the charge mobility is much more sensitive to the variation of the spatial wave function overlap between Mn–O–Mn orbitals than the relative spin angle between neighbouring Mn ions. At lower temperatures, the effect of the magnetic field and pressure on electrical transport is negligible in spite of the presence of very different magnetic domain structures.

Acknowledgments

We are indebted to J J Neumeier for useful discussions. This work was supported by the Brazilian agencies FAPESP under Grant Nos 05/53241-9 and 07/01039-7 and CNPq under Grant No 473932/2007-5.

References

- [1] Dagoto E, Hotta T and Moreo A 2001 *Phys. Rep.* **344** 1
- [2] Cheong S-W and Hwang H Y 1999 *Colossal Magnetoresistance Oxides* (ed Y Tokura) (London: Gordon and Breach)
- [3] Souza J A, Yu Y-K, Neumeier J J, Terashita H and Jardim R F 2005 *Phys. Rev. Lett.* **94** 207209
- [4] Souza J A, Terashita H, Granado E, Jardim R F, Muccillo R and Oliveira N F Jr. 2008 *Phys. Rev. B* **78** 054411
- [5] Zener C 1951 *Phys. Rev.* **82** 403
- [6] de Gennes P G 1960 *Phys. Rev.* **118** 141
- [7] Anderson P W and Hasegawa H 1955 *Phys. Rev.* **100** 675
- [8] Medarde M, Mesot J, Lacorre P, Rosenkranz S, Fischer P and Gobrecht K 1995 *Phys. Rev. B* **52** 9248
- [9] Neumeier J J, Hundley M F, Thompson J D and Heffner R H 1995 *Phys. Rev. B* **52** 7006
- [10] Escote M T, da Silva A M L, Matos J R and Jardim R F 2000 *J. Solid State Chem.* **151** 298
- [11] Souza J A, Neumeier J J and Jardim R F 2007 *Phys. Rev. B* **75** 012412
- [12] Coey J M D, Viret M, von Molnar S 1998 *Adv. Phys.* **48** 167
- [13] Laukhin V, Fontcuberta J, Garcia-Munoz J L and Obradors X 1997 *Phys. Rev. B* **56** R10009
- [14] Mira J, Rivas J, Hueso L E, Rivadula F, Lopez Quintela M A, Senaris Rodrigues M A and Ramos C A 2001 *Phys. Rev. B* **65** 024418
- [15] Postorino P, Congeduti A, Dore P, Sacchetti A, Gorelli F, Ulivi L, Kumar A and Sarma D D 2003 *Phys. Rev. Lett.* **91** 175501
- [16] Jaime M, Hardner H T, Salamon M B, Rubinstein M, Dorsey P and Emin D 1997 *Phys. Rev. Lett.* **78** 951
- [17] Lorenz B, Heilman A K, Wang Y S, Xue Y Y and Chu C W 2001 *Phys. Rev. B* **63** 144405
- [18] Souza J A, Neumeier J J and Yi-Kuo Yu 2008 *Phys. Rev. B* **78** 014436
- [19] Moreo A, Mayr M, Feiguin A, Yunoki S and Dagotto E 2000 *Phys. Rev. Lett.* **84** 5568
- [20] Mayr M, Moreo A, Verges J, Arispe J, Feiguin A and Dagotto E 2001 *Phys. Rev. Lett.* **86** 135
- [21] Goya G F, Souza J A and Jardim R F 2002 *J. Appl. Phys.* **91** 7932
- [22] Hundley M F, Hawley M, Heffner R H, Jia Q X, Neumeier J J, Tesmer J, Thompson J D and Wu X D 1995 *Appl. Phys. Lett.* **67** 860
- [23] Hwang H Y, Cheong S W, Ong N P and Batlogg B 1996 *Phys. Rev. Lett.* **77** 2041
- [24] Martinez B, Balcells L, Fontcuberta J, Obradors X, Cohenca C H and Jardim R F 1998 *J. Appl. Phys.* **83** 7058
- [25] Zhang S and Yang Z 1996 *J. Appl. Phys.* **79** 7398
- [26] Loa I, Adler P, Grzechnik A, Syassen K, Schwarz U, Hanfland M, Rozenberg G Kh, Gorodetsky P and Pasternak M P 2001 *Phys. Rev. Lett.* **87** 125501
- [27] Fuhr J D, Avignon M and Alascio B 2008 *Phys. Rev. Lett.* **100** 216402